



The effects of dielectric shield on specific absorption rate and heat transfer in the human body exposed to leakage microwave energy[☆]

Teerapot Wessapan, Siramate Srisawatdhisukul, Phadungsak Rattanadecho^{*}

Research Center of Microwave Utilization in Engineering (R.C.M.E.), Department of Mechanical Engineering, Faculty of Engineering, Thammasat University (Rangsit Campus), Pathumthani 12120, Thailand

ARTICLE INFO

Available online 16 December 2010

Keywords:

Microwave energy
Numerical methods
SAR
Heat transfer analysis
Dielectric shield

ABSTRACT

This paper proposes a numerical study to simulate the effects of dielectric shield on the specific absorption rate (SAR) and the temperature increase in the human body exposed to leakage microwave energy. In this study, the effects of shield dielectric properties on distributions of SAR and temperature increase within the human body at various operating frequency are systematically investigated. Based on the obtained results, the installed dielectric shield strongly affects the SAR and the temperature increase in human body. The SAR and the temperature increase in human body can be reduced simultaneously by setting the appropriate dielectric properties of the dielectric shield. The appropriate dielectric properties of the dielectric shield greatly depend on the operating frequencies. These fundamental data for the implementations of the radiation protection shielding materials, with focusing on the human organism, are provided as well.

© 2010 Elsevier Ltd. All rights reserved.

1. Introduction

Microwave is a form of electromagnetic wave with wavelengths ranging from 1 m down to 1 mm, with frequencies between 0.3 and 300 GHz. Microwave energy has proven to be an efficient and reliable form of heating for a wide range of industrial processes such as heating process [1], curing process [2], and melting process [3]. As applications of microwave energy become widespread, adverse effects caused by the leakage microwave energy are increasingly a subject of concern [4,5]. In many countries, various studies on biological effects have been made and many results have been reported. There has been an intensive model analysis of the SAR of the human body [6,7]. The protection is serious for researchers who work with high-power electromagnetic waves. In connection with research on human protection from electromagnetic field exposure, some researches have been carried out on how effectively the human body is protected from unwanted electromagnetic waves [8]. Furthermore, fundamental analysis of shielding effects of lossy dielectric materials located in front of a human body have also been carried out by some researchers [9,10]. However, the heat transfer model has not been included in the modeling analysis.

The computation of the temperature increase is one of the main tasks in the evaluation of the risk related to the exposure of humans to electromagnetic fields [11]. Nevertheless, most studies of human protection from electromagnetic field exposure have not considered the temperature increase within the domain of the human body

especially in the human organism. There are few studies on the temperature and electromagnetic field interaction in a realistic physical model of the human body due to the complexity of the problem, even though it is directly related to the thermal injury of tissues [7,12,13]. Therefore, in order to provide information on protection of the human body against electromagnetic fields adequately, it is essential to simulate the coupled electromagnetic field and heat transfer models to represent an actual process of shield protection from possibly harmful effects of electromagnetic fields. This research is a pioneer work on human protection from electromagnetic field exposure that simulates the SAR distribution and temperature distribution over an anatomically based human body.

This work is extended from our previous work [7] in which the human body exposed to leakage electromagnetic field is investigated. This paper mainly analyzes the shielding effect of a dielectric shield being placed in front of a human body. Specifically, lossy dielectric media are chosen as the dielectric shield material. The local SARs and temperature increase of human model are calculated for various operating frequencies. Three shield dielectric properties at microwave frequencies of 300, 915, 1300, and 2450 MHz are selected for the shielding investigation. The system of governing equations, as well as initial and boundary conditions are solved numerically, using finite element method (FEM). Moreover, this research is also focusing on the interaction between electromagnetic field and organs in the human trunk.

2. Formulation of the problem

Fig. 1 depicts a physical model of the problem. The incident plane wave (TE wave) with a microwave power density of 5 mW/cm^2 is

[☆] Communicated by W.J. Minkowycz.

^{*} Corresponding author.

E-mail address: ratphadu@engr.tu.ac.th (P. Rattanadecho).

Nomenclatures	
C_p	specific heat capacity (J/(kg K))
E	electric fields intensity (V/m)
f	frequency of incident wave (Hz)
k	thermal conductivity (W/m K)
H	magnetic field intensity (A/m)
n	refractive index (-)
Q	heat generation term (W/m ³)
s	Poynting vector (W/m ²)
T	temperature (°C)
t	time (s)
$\tan \delta$	dielectric loss coefficient (-)
Greek letters	
ϵ	permittivity (F/m)
μ	magnetic permeability (H/m)
v	velocity of propagation (m/s)
ρ	density (kg/m ³)
σ	electric conductivity (S/m)
ω	perfusion rate (1/s)
Subscript	
b	blood
ext	external
met	metabolism

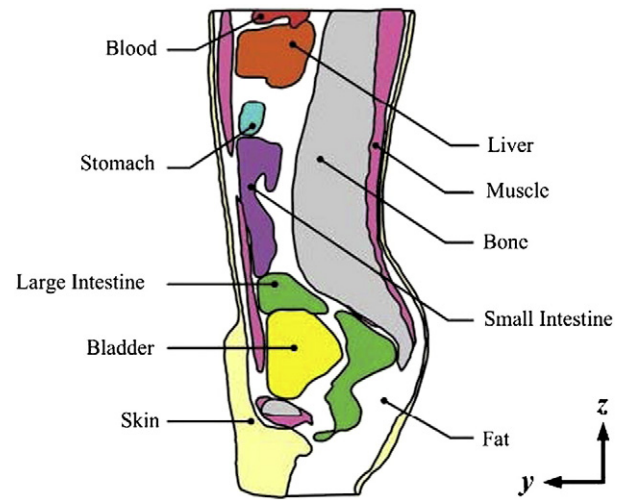


Fig. 2. Human body in vertical cross section plane [12].

of Shiba and Higaki [12]. The human model has a dimension of 300 mm in width and 525 mm in height. This human model comprises 10 types of tissues which are the skin, fat, muscle, bone, large intestine, small intestine, bladder, blood, stomach, and liver, respectively. These tissues have different dielectric and thermal properties. The thermal properties and dielectric properties of these tissues at the frequencies of 300, 915, 1300, and 2450 MHz are given in Table 1 and Table 2, respectively.

incident on the dielectric shield in front of the human model and penetrated into the human model. A human model including ten kinds of organs is used for our analysis.

2.1. Human model

Fig. 2 shows a vertical cross section through the middle plane of the human trunk model. A two-dimensional human body model used in this paper is obtained by image processing technique from the work

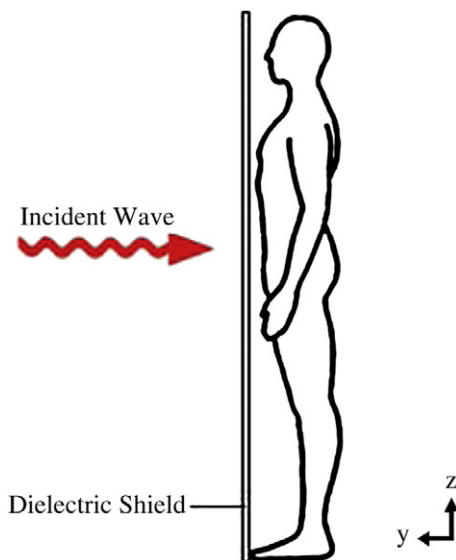


Fig. 1. Human model with dielectric shield.

2.2. Modeling of electromagnetic fields

A mathematical model is developed to calculate the electric field, SAR, and temperature distribution within the human model. To simplify the problem, the following assumptions are made; electromagnetic wave propagation is modeled in two dimensions over the y-z plane, in which waves and object interaction proceed in the open region, and the computational space is truncated by scattering boundary condition. The propagation of an electromagnetic wave is characterized by transverse electric fields (TE-Mode). The dielectric properties of human tissues are frequency dependent as shown in Table 1. Since the temperature increase in the human model is slightly changed, the model assumes that the dielectric properties of tissues are independent to temperature change for the specified frequency.

The electromagnetic wave propagation is calculated by Maxwell's equations [6], which mathematically describe the interdependence of

Table 1 Dielectric properties of tissues.

Tissue	300 MHz		915 MHz		1300 MHz		2450 MHz	
	σ (S/m)	ϵ_r						
Skin	0.35	48.41	0.92	44.86	1.25	43.56	2.16	41.79
Fat	0.06	6.55	0.09	5.97	0.10	5.80	0.13	5.51
Muscle	1.08	55.45	1.33	50.44	1.42	48.96	1.60	46.40
Bone	2.10	44.80	2.10	44.80	2.10	44.80	2.10	44.80
Large intestine	2.04	53.90	2.04	53.90	2.04	53.90	2.04	53.90
Small intestine	3.17	54.40	3.17	54.40	3.17	54.40	3.17	54.40
Bladder	0.69	18.00	0.69	18.00	0.69	18.00	0.69	18.00
Blood	2.54	58.30	2.54	58.30	2.54	58.30	2.54	58.30
Stomach	2.21	62.20	2.21	62.20	2.21	62.20	2.21	62.20
Liver	1.69	43.00	1.69	43.00	1.69	43.00	1.69	43.00

Table 2
Thermal properties of tissues.

Tissue	ρ (kg/m ³)	k (W/m · K)	C_p (J/kg · K)	ω_b	Q_{met} (W/m ³)
Skin	1125	0.35	3437	0.02	1620
Fat	916	0.22	2300	4.58E-04	300
Muscle	1047	0.6	3500	8.69E-03	480
Bone	1038	0.436	1300	4.36E-04	610
Large intestine	1043	0.6	3500	1.39E-02	9500
Small intestine	1043	0.6	3500	1.74E-02	9500
Bladder	1030	0.561	3900	0.00E+00	–
Blood	1058	0.45	3960	–	–
Stomach	1050	0.527	3500	7.00E-03	–
Liver	1030	0.497	3600	0.017201	–

the electromagnetic waves. The general form of Maxwell's equations is simplified to demonstrate the electromagnetic field of microwave penetrated into the human model as the following equations:

$$\nabla \times \left(\frac{1}{\mu_r} \nabla \times E \right) - k_0^2 \left(\epsilon_r - \frac{j\sigma}{\omega\epsilon_0} \right) E = 0 \quad (1)$$

$$\epsilon_r = n^2 \quad (2)$$

where E is electric field intensity (V/m), μ_r is relative magnetic permeability (H/m), n is refractive index, ϵ_r is relative dielectric constant, $\epsilon_0 = 8.8542 \times 10^{-12}$ (F/m) is permittivity of free space, and σ is electric conductivity (S/m), $j = \sqrt{-1}$.

2.2.1. Boundary condition for wave propagation analysis

Microwave energy is emitted by a microwave high power device and strikes the dielectric shield in front of the human model with a microwave power density of 5 mW/cm². The microwave power density in terms of mW/cm² in 2D model can be presumed by dividing the microwave power (mW) by a frontal area of the incident microwave (cm²). Therefore, boundary conditions used for electromagnetic wave, as shown in Fig. 3, are considered in the following.

It is assumed that the uniform wave flux strikes the left side of the human model, where the dielectric shield is located and then penetrates into the human model. From the viewpoint of convergence of the electromagnetic field, only the TE wave is used as the incident wave. Therefore, at the left boundary of the considered domain, an electromagnetic simulator employs TE wave propagation port with specified power density:

$$S = \int (E - E_1) \cdot E_1 / \int E_1 \cdot E_1 \quad (3)$$

Boundary conditions along the interfaces between different mediums, for example, between air and tissue or tissue and tissue (with different dielectric properties), are considered as continuity boundary condition:

$$n \times (H_1 - H_2) = 0 \quad (4)$$

The outer sides of the tissue boundaries are considered as scattering boundary condition:

$$n \times (\nabla \times E_z) - jkE_z = -jk(1 - k \cdot n)E_{0z} \exp(-jk \cdot r) \quad (5)$$

2.3. Interaction of electromagnetic waves and human tissues

Interaction of electromagnetic fields with biological tissues can be defined in terms of the SAR. When EM waves propagate through the dielectric shield and then penetrate into the human tissues, the energy of EM waves is absorbed by the tissues. The SAR is defined as the power dissipation rate normalized by tissue density [14]. The SAR is given by:

$$SAR = \frac{\sigma}{\rho} |E|^2 \quad (6)$$

where E is the root mean square electric-field (V/m), σ is the conductivity (S/m) and ρ is mass density of the tissue (kg/m³).

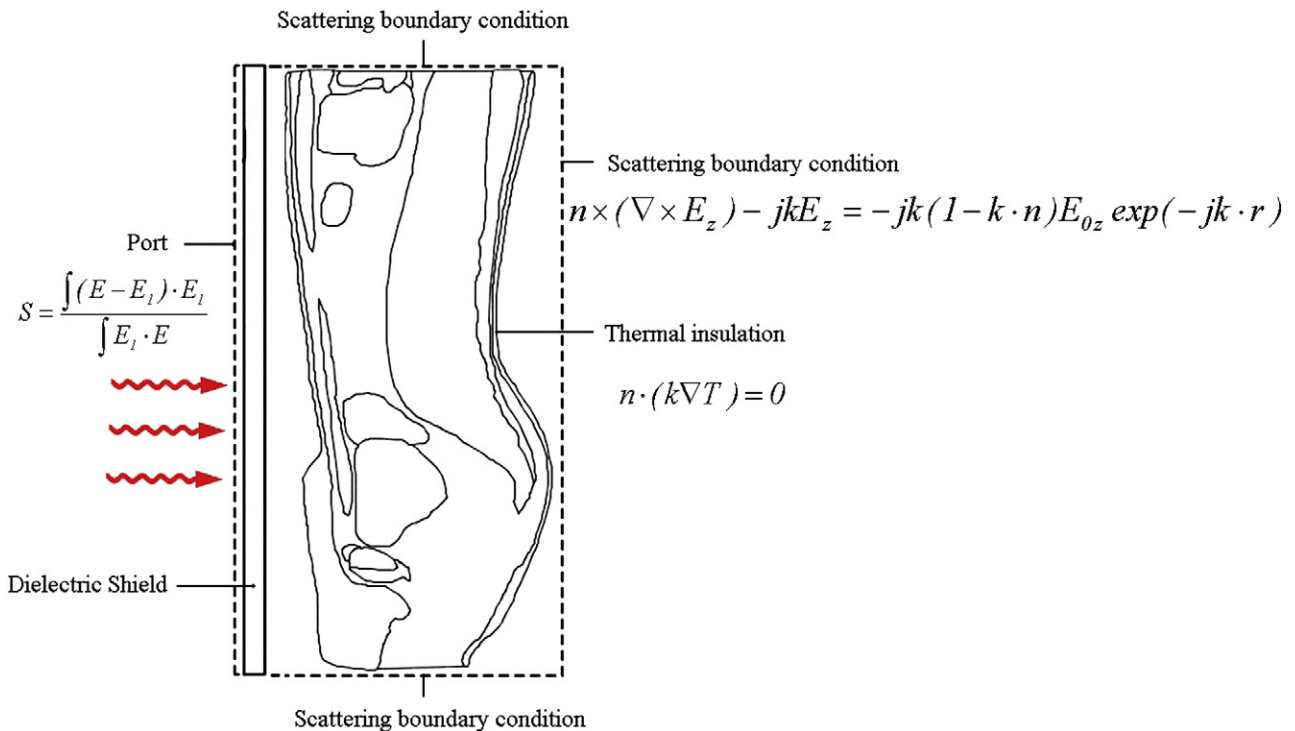


Fig. 3. Physical model and boundary condition used for analysis.

2.4. Modeling of heat transfer

The heat transfer analysis is considered only in the human body domain, which does not include parts of the surrounding space as well as the dielectric shield. To reduce complexity of the problem, the following assumptions have been introduced.

1. There is no phase change and mass transfer in the human model.
2. The human tissues are bio-material with constant thermal properties.
3. There is no chemical reactions occurring within the human model.
4. The initial temperature through the human model is uniform.

The heat transfer analysis of the human model is modeled in two dimensions over the y–z plane. The temperature distribution inside the human model is obtained by using the Pennes' bio-heat equation [15]. The transient bioheat equation effectively describes how heat transfer occurs within the human model, and the equation can be written as:

$$\rho C \frac{\partial T}{\partial t} = \nabla \cdot (k \nabla T) + \rho_b C_b \omega_b (T_b - T) + Q_{met} + Q_{ext} \tag{7}$$

where ρ is the tissue density (kg/m^3), C is the heat capacity of tissue ($\text{J/kg} \cdot \text{K}$), k is thermal conductivity of tissue ($\text{W/m} \cdot \text{K}$), T is the temperature ($^{\circ}\text{C}$), T_b is the temperature of blood flow ($^{\circ}\text{C}$), ρ_b is the density of blood before entering ablation region (kg/m^3), C_b is the specific heat capacity of blood ($\text{J/kg} \cdot \text{K}$), ω_b is the blood perfusion rate ($1/\text{s}$), Q_{met} is the metabolism heat source (W/m^3) and Q_{ext} is the external heat source (microwave heat-source density) (W/m^3).

In the analysis, heat conduction between tissue and blood flow is approximated by the term $\rho_b C_b \omega_b (T_b - T)$. In this analysis, the thermoregulation mechanisms and the metabolic heat generation of each tissue have been neglected to illustrate the clear temperature distribution. The metabolism heat source is negligible and therefore $Q_{met} = 0$.

The external heat source is equal to the resistive heat generated by electromagnetic field (microwave power absorbed):

$$Q_{ext} = \frac{1}{2} \sigma_{tissue} |\vec{E}|^2 \tag{8}$$

where $\sigma_{tissue} = 2\pi f \epsilon_r' \epsilon_0$.

2.4.1. Boundary condition for heat transfer analysis

At the skin–air interface, the insulated boundary condition has been imposed to clearly illustrate the temperature distribution. As shown in Fig. 3, the boundaries of human body are considered as insulated boundary condition:

$$n \cdot (k \nabla T) = 0. \tag{9}$$

Table 3
Dielectric properties of shield and penetration depth.

Operating frequency (MHz)	D_p (cm)		
	Low lossy 10-j5	Medium lossy 10-j10	High lossy 20-j20
300	10.36	5.53	3.91
915	3.40	1.81	1.28
1300	2.39	1.28	0.90
2450	1.27	0.68	0.48

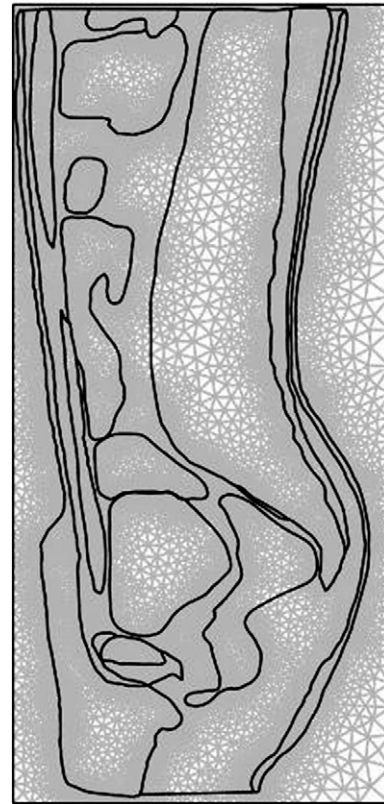


Fig. 4. A two-dimensional finite element mesh of human cross section model.

It is assumed that no contact resistant occurs between the internal organs of the human body. Therefore, the internal boundaries are assumed to be in a continuity boundary condition between the tissue layers within the human model:

$$n \cdot (k_u \nabla T_u - k_d \nabla T_d) = 0. \tag{10}$$

2.4.2. Initial condition for heat transfer analysis

For this analysis, the temperature distribution within the human body is assumed to be uniform. Therefore, initial temperature of human body is defined as

$$T(t_0) = 37^{\circ}\text{C}. \tag{11}$$

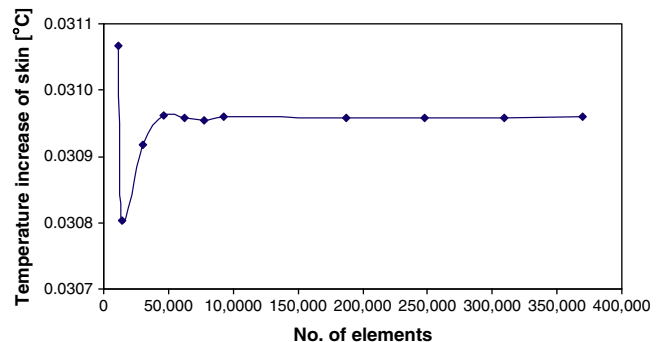


Fig. 5. Grid convergence curve of the 2D model.

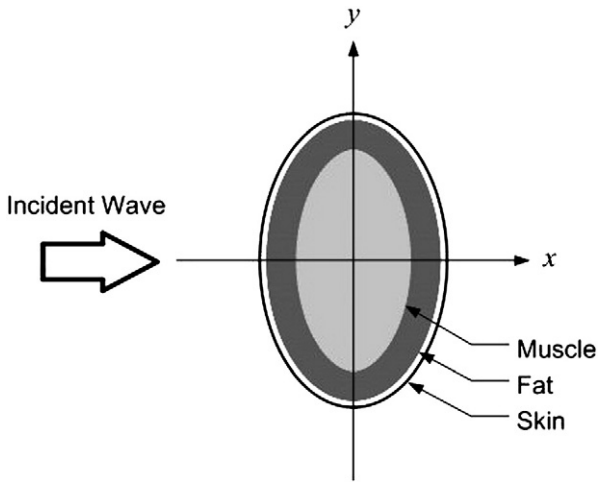


Fig. 6. Geometry of the validation model [9].

2.5. Penetration depth

The penetration depth (D_p) is defined as the distance at which the microwave power density has decreased to 37% of its initial value at the surface [16]:

$$D_p = \frac{1}{\frac{2\pi f}{v} \sqrt{\frac{\epsilon_r' \left(\sqrt{1 + \left(\frac{\epsilon_r''}{\epsilon_r'}\right)^2} - 1 \right)}{2}}} = \frac{1}{\frac{2\pi f}{v} \sqrt{\frac{\epsilon_r' \left(\sqrt{1 + (\tan\delta)^2} - 1 \right)}{2}}} \tag{12}$$

where ϵ_r'' is the relative dielectric loss factor and v is the speed of microwave (m/s).

The penetration depth of the microwave power is calculated using Eq. (12), which shows how it depends on the dielectric properties of the dielectric material. The shield dielectric properties and the penetration depth of the dielectric shield are summarized in Table 3.

It is shown that the D_p is greatly dependent on the shield dielectric properties as well as the operating frequency. With high lossy of dielectric shield typically shows greater potential for absorbing

microwaves in dielectric shield, while an increase in operating frequency typically decreases in D_p .

3. Numerical procedure

The coupled model of bioheat equation and Maxwell's equation are used to simulate the SAR and temperature increase in the human model. The computational scheme is to first assemble a finite element model and compute a local heat generation term by performing an electromagnetic calculation using tissue properties. In order to obtain a good approximation, a fine mesh is specified in the sensitive areas. This study provides a variable mesh method for solving the problem as shown in Fig. 4. The coupled model of electromagnetic field and thermal field is solved by FEM. The model is implemented using COMSOL™ Multiphysics 3.4, to demonstrate the phenomenon that occurs within the human body exposed to leakage microwave energy. The study employs an implicit time step scheme to solve the electric field and temperature field. The 2D model is discretized using triangular elements and the Lagrange quadratic is used to approximate the temperature and SAR variation across each element. Convergence test of the frequency of 2450 MHz are carried out to identify the suitable number of elements required. The number of elements where solution is independent of mesh density is found to be 92,469. The convergence curve resulting from the convergence test is shown in Fig. 5.

4. Results and discussion

In this section, the couple of the mathematical model of bioheat transfer and electromagnetic wave propagation as well as an initial temperature of 37 °C for all cases is used for the analysis. For the simulation, the thermal properties and dielectric properties are directly taken from Table 1 to Table 3, respectively. The influences of shield dielectric properties and operating frequency on SAR and temperature increase within the human model are clearly investigated.

4.1. Numerical validations

It must be noted in advance that it is not possible to make a direct comparison of the model in this study and the experimental results due to the medical ethics. In order to verify the accuracy of the present numerical model, the simple case of the simulated results is then validated against the numerical results with the same geometric

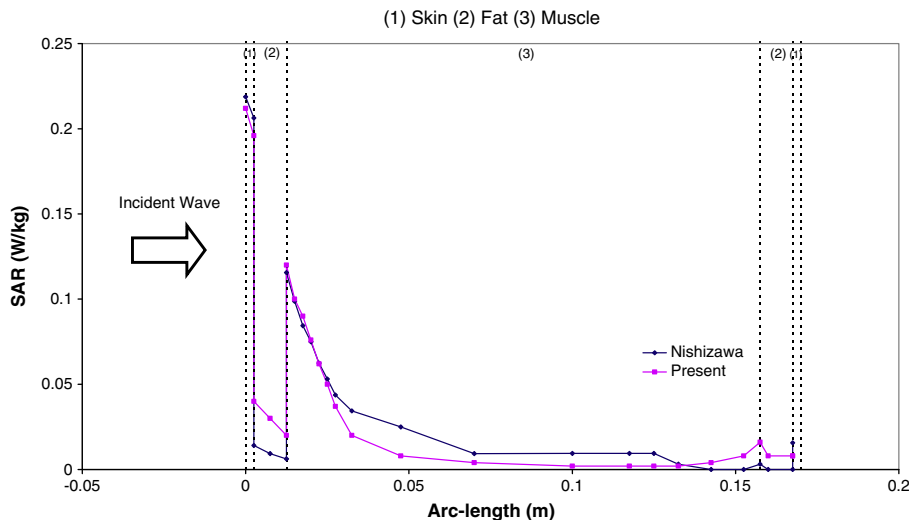


Fig. 7. Comparison of the calculated SAR distribution to the SAR distribution obtained by Nishizawa et al. [9].

Table 4
Comparison of the results obtained in the present study with those of Nishizawa et al. [9].

	Present work	Published work [9]	% Difference
SAR _{max} in skin	0.212	0.220	3.63
SAR _{max} in fat	0.198	0.206	3.88
SAR _{max} in muscle	0.116	0.120	3.33

model presented by Nishizawa et al. [9]. The horizontal cross section of the three layer human tissues as shown in Fig. 6 is used in the validation case. In the validation case, the leakage microwave power density of 1 mW/cm² at the electromagnetic frequency of 1300 MHz is considered. The results of the selected test case are illustrated in Fig. 7 for SAR distribution in the human body. Table 4 clearly shows a good agreement of the maximum value of the SAR of tissue between the present solution and that of Nishizawa [9]. This favorable comparison lends confidence in the accuracy of the present numerical model. It is important to note that there may be some errors occurring in the simulations which are generated by the input dielectric properties data base and the numerical scheme.

4.2. The effects of shield dielectric properties and operating frequency

Fig. 8 shows the meshes of the human model as well as the SAR and temperature distribution in the case of unshielded human model exposed to the microwave power density of 5 mW/cm² at the frequency of 300 MHz. It is found that the temperature distributions are not proportional to the local SAR values. Nevertheless, these are also related to the parameters such as thermal conductivity, dielectric properties, blood perfusion rate and etc.

In the case of using dielectric shield, the dielectric properties for the shield are chosen as (low-loss; 10-j5), (medium-loss; 10-j10), and (high-loss; 20-j20). The shield gap distance and shield thickness are set to 0.5 cm and 0.3 cm, respectively. Fig. 9 and Fig. 10 show the maximum SAR and maximum temperature increase, respectively, in the human model with the test frequencies of 300 MHz, 915 MHz, 1300 MHz and 2450 MHz.

In this section, we illustrate the maximum value of SAR and temperature increase in the human model without attention to the organism. In the unshielded case, the maximum SAR value appeared at 1300 MHz as shown in Fig. 9, while the maximum temperature increase appeared at 915 MHz as shown in Fig. 10. This is because the

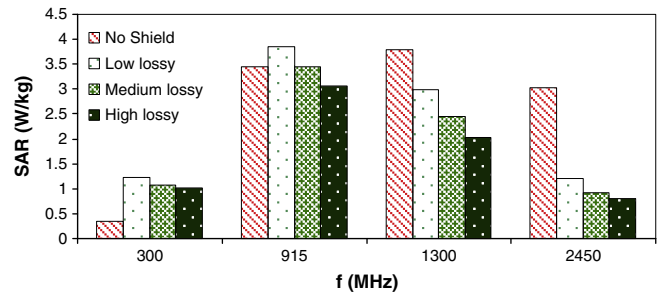


Fig. 9. Comparison of the maximum SAR in the human model at the frequencies of 300 MHz, 915 MHz, 1300 MHz and 2450 MHz.

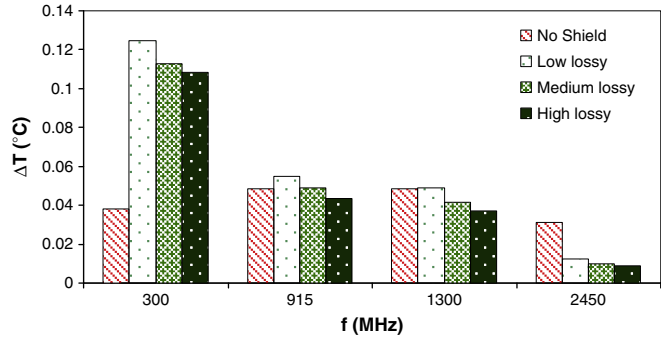


Fig. 10. Comparison of the maximum temperature increases in the human model at the frequencies of 300 MHz, 915 MHz, 1300 MHz and 2450 MHz.

differences of dielectric and thermal properties of tissues cause spatial distortions of the resonance excitation.

Since in this study, the thickness of the dielectric shield is less than the penetration depth, only a part of the supplied microwave energy is absorbed by the dielectric shield, and the other parts are allowed to penetrate further through the dielectric shield. This causes the interference of waves to penetrate further into the human model to be reflected from the human skin and travel back to the dielectric shield. Consequently, the reflection and transmission components at each interface contribute to the resonance of standing wave within the gap and the human model.

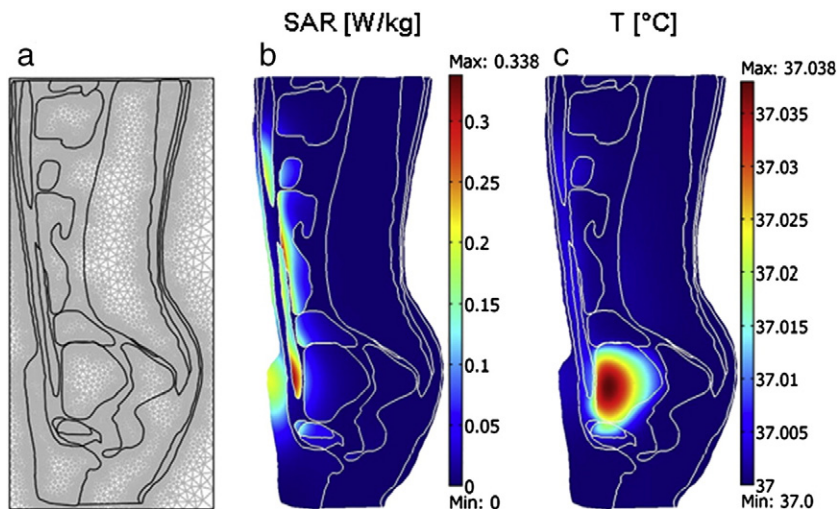


Fig. 8. Analysis of SAR and temperature distribution in the human model exposed to the microwave power density of 5 mW/cm² at the frequency of 300 MHz, (a) An initial finite element meshes of human cross section model (b) SAR distribution of the shieldless case (c) Temperature distribution of the unshield case.

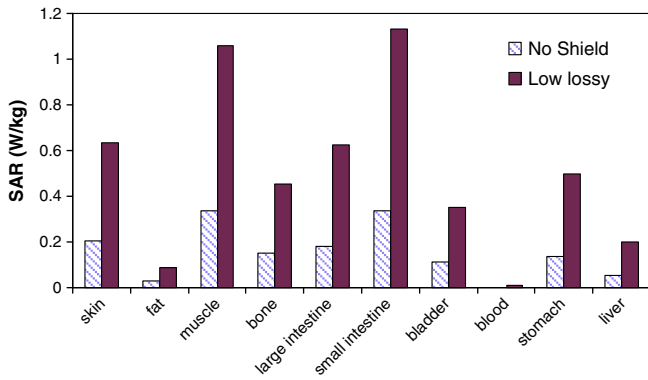


Fig. 11. Comparison of the maximum SAR in human organs of the unshielded and shielded human model at the frequency of 300 MHz.

It is evident from Fig. 9 and Fig. 10 that in the higher frequency of 1300 and 2450 MHz, when using dielectric shield, a significant reduction of SAR and temperature increase within the human model is achieved because of its smaller penetration depth. However, in the lower frequency of 300 MHz corresponding to a long wavelength, the SAR and the temperature increase have higher value than the values of the unshielded case. The reason behind this result is that the penetration depth of the dielectric shield at 300 MHz is much greater than the dielectric shield thickness. This increases a larger part of the incident wave to penetrate further through the dielectric shield and also penetrate into the human model. The great value of SAR and temperature increase in human model is caused by stronger resonance effects that occur at the low frequencies.

While in the frequency of 915 MHz, an insignificant shielding effect of medium lossy dielectric shield is illustrated. It is found that by using low lossy dielectric shield at the frequency of 915 MHz, SAR as well as temperature increase is higher compared to values of the unshielded case. This is because the resonance phenomena between the low lossy dielectric shield and human model is displayed stronger. The multiple reflections within the gap and the human model caused the accumulation of microwave energy in the gap which leads to an increase in the SAR and temperature in human organism by which the reflection rate of microwave strongly depends on the dielectric properties of the dielectric shield. By using the high lossy dielectric shield, the shielding effect is significant. This is because of a large reduction of microwave power density within the human model due to the weakness of resonance, corresponding to the lowering penetration depth of microwave. It is confirmed that the appropriate dielectric properties of the dielectric shield greatly depend on the operating frequencies.

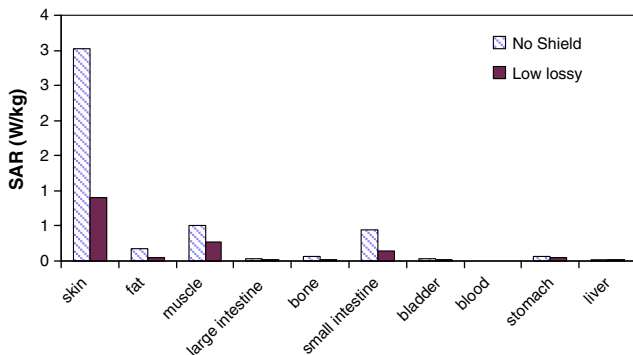


Fig. 12. Comparison of the maximum SAR in human organs of the unshielded and shielded human model at the frequency of 2450 MHz.

4.3. SAR in organs

As shown in Fig. 11, based on the results of the local maximum SAR of the unshielded case, at a low frequency of 300 MHz, peak values of SAR occurred, found both in the small intestine and the muscle. With the use of the low lossy shield, the greater values of SAR occurred as compared to the unshielded case. This is because of a larger part of the incident wave that penetrates further into the gap and human model. This caused the accumulation of microwave energy in the gap and the human model. Fig. 12 shows the maximum SAR in organs at a high frequency of 2450 MHz. It is clearly evident from Fig. 12 that a peak value of local SAR is found only at the skin due to a smaller penetration depth at high frequency range. However, large reduction of the SAR value is achieved when using the same dielectric shield (low-loss shield) with the case of 300 MHz due to the weakness of resonance.

Fig. 11 and Fig. 12 show the maximum SAR and the maximum temperature increase in the human model, while focusing on the human organism. It is found that the SAR and the temperature increase primarily depend on the penetration depth of microwave which corresponds to the operating frequency as well as the dielectric properties of the dielectric shield. As the dielectric properties of a dielectric shield vary, the penetration depth will be changed and the electric field passing through the dielectric shield is altered. If the penetration depth is changing, a fraction of the microwave energy absorbed is also changed which related to the resonance within the model. Consequently, the shielding effect of dielectric shield is changed.

5. Conclusions

This paper presents the simulations of SAR and heat transfer in the human model, where microwave energy strikes the dielectric shield in front of the human model. The SAR and temperature distributions in the human model are governed by the electric field as well as the dielectric properties of tissue.

The results show an interaction between physical parameters: operating frequencies and shield dielectric properties. For human exposure to microwave energy, the installed dielectric shield strongly affects the SAR and the temperature increase in the human body. Actually, the microwaves can transmit through the dielectric shield, and can penetrate into the human model that contribute to the resonance of standing wave within the gap and human model.

Since the frequency increases, the penetration depth for microwave gets smaller and resonance effect becomes weakness. Consequently, the shielding effect is significant. Therefore, the appropriate dielectric properties, which can effectively reduce the SAR and the temperature increase in human body of the dielectric shield, are greatly dependent on the operating frequency. Additionally, this paper presents an interesting viewpoint on the microwave shielding properties of dielectric shields at various operating frequencies, while focusing on the human organism.

Future work will extend the calculations of the SAR and the temperature increase for a three-dimensional model. Moreover, it will be carried out to study the effect of wave pattern, namely, TM wave and TE wave on a realistic model.

Acknowledgments

The authors gratefully acknowledge the financial support provided by The Thailand Research Fund (TRF), and the authors also acknowledge Thammasat University for providing the simulation facilities described in this paper.

References

- [1] P. Ratanadecho, N. Suwannapum, W. Cha-um, Interactions between electromagnetic and thermal fields in microwave heating of hardened type I-cement paste using a rectangular waveguide (influence of frequency and sample size), *ASME Journal of Heat Transfer* 131 (2009) 082101–082112.
- [2] N. Makul, P. Ratanadecho, Microwave pre-curing of natural rubber-compounding using a rectangular wave guide, *International Communications in Heat and Mass Transfer* 37 (7) (2010) 914–923.
- [3] P. Ratanadecho, C. Sertikul, Simulation of melting of ice under a constant temperature heat source using a combined transfinite interpolation and partial differential equation methods, *Journal of Porous Media* 10 (7) (2007) 657–675.
- [4] M.A. Stuchly, Health effects of exposure to electromagnetic fields, *IEEE Aerospace Applications Conference Proceedings*, Aspen, USA, 1995, pp. 351–368.
- [5] K.L. Ryan, J.A. D'Andrea, J.R. Jauchem, P.A. Mason, Radio frequency radiation of millimeter wave length: Potential occupational safety issues relating to surface heating, *Health Physics* 78 (2000) 170–181.
- [6] R.J. SPIEGEL, A review of numerical models for predicting the energy deposition and resultant thermal response of humans exposed to electromagnetic fields, *IEEE Transactions on Microwave Theory and Techniques* 32 (1984) 730–746.
- [7] T. Wessapan, S. Srisawatdhisukul, P. Rattanadecho, Numerical analysis of specific absorption rate and heat transfer in the human body exposed to leakage electromagnetic field at 915 MHz and 2,450 MHz, *ASME Journal of Heat Transfer*, xx (2011) xxx-xxx. (Accepted).
- [8] A.W. Guy, C.-K. Chou, J.A. McDougall, C. Sorensen, Measurement of shielding effectiveness of microwave-protective suits, *IEEE Transactions on Microwave Theory and Techniques* 35 (1987) 984–994.
- [9] S. Nishizawa, O. Hashimoto, Effectiveness analysis of lossy dielectric shields for a three-layered human model, *IEEE Transactions on Microwave Theory and Techniques* 47 (1999) 277–283.
- [10] O. Hashimoto, S. Nishizawa, Effectiveness analysis of thin resistive sheet for a three-layered elliptical human model, *Microwave and Optical Technology Letters* 23 (1999) 73–75.
- [11] T. Samaras, A. Christ, A. Klingenbck, N. Kuster, Worst case temperature rise in a one-dimensional tissue model exposed to radiofrequency radiation, *IEEE Transactions on Biomedical Engineering* 54 (2007) 492–496.
- [12] K. Shiba, N. Higaki, Analysis of SAR and current density in human tissue surrounding an energy transmitting coil for a wireless capsule endoscope, *Proceedings of the 20th International Zurich Symposium on Electromagnetic Compatibility* 1 (2009) 321–324, Zurich.
- [13] A. Hirata, O. Fujiwara, T. Shiozawa, Correlation between peak spatial-average SAR and temperature increase due to antennas attached to human trunk, *IEEE Transactions on Biomedical Engineering* 53 (2006) 1658–1664.
- [14] A. Hirata, M. Fujimoto, T. Asano, J. Wang, O. Fujiwara, T. Shiozawa, Correlation between maximum temperature increase and peak SAR with different average schemes and masses, *IEEE Transactions on Electromagnetic Compatibility* 48 (2006) 569–577.
- [15] D. Yang, M.C. Converse, D.M. Mahvi, J.G. Webster, Expanding the bioheat equation to include tissue internal water evaporation during heating, *IEEE Transactions on Biomedical Engineering* 54 (2007) 1382–1388.
- [16] T. Basak, K. Aparna, A. Meenakshi, A.R. Balakrishnan, Effect of ceramic supports on microwave processing of porous food samples, *International Journal of Heat and Mass Transfer* 49 (2006) 4325–4339.